eLIFE
elifesciences.org

Figures and figure supplements

Transport of soluble proteins through the Golgi occurs by diffusion via continuities across cisternae

Galina V Beznoussenko, et al.

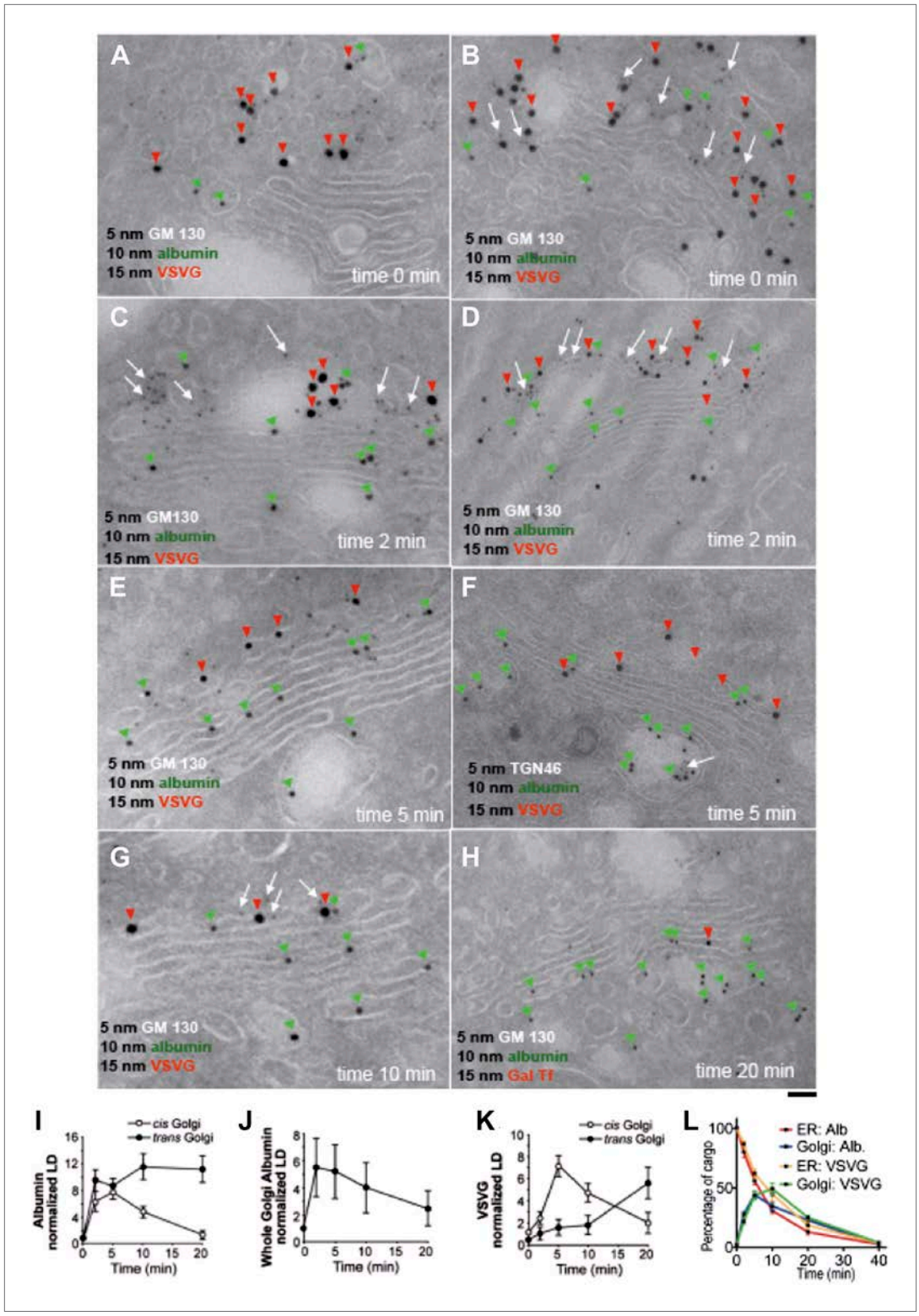

Figure 1. Kinetic patterns of synchronized transport of albumin and VSVG through the Golgi stack. VSV-infected HepG2 cells were synchronized according to the CHX/32-15°C protocol ('Materials and methods'). Following release of the 15°C block, the cells were examined by immuno-EM (**A**–**H**) at the indicated times. Panels (**I**–**K**) show quantification of immuno-EM values as labeling density (LD) normalized to the density in the ER, to avoid labeling variability across samples. (**L**) The amount of albumin or VSVG in indicated compartments were normalized to that

Figure 1. Continued on next page

Figure 1. Continued

present at time 0 in the ER and expressed as percentage. Values are mean ± SD from 30 stacks per time point, in three independent experiments for immuno-EM. Bar: 60 nm (**A**), 50 nm (**B**, **C**, **E**, **G**), 100 nm (**D**, **H**), 80 nm (**F**).

DOI: 10.7554/eLife.02009.003

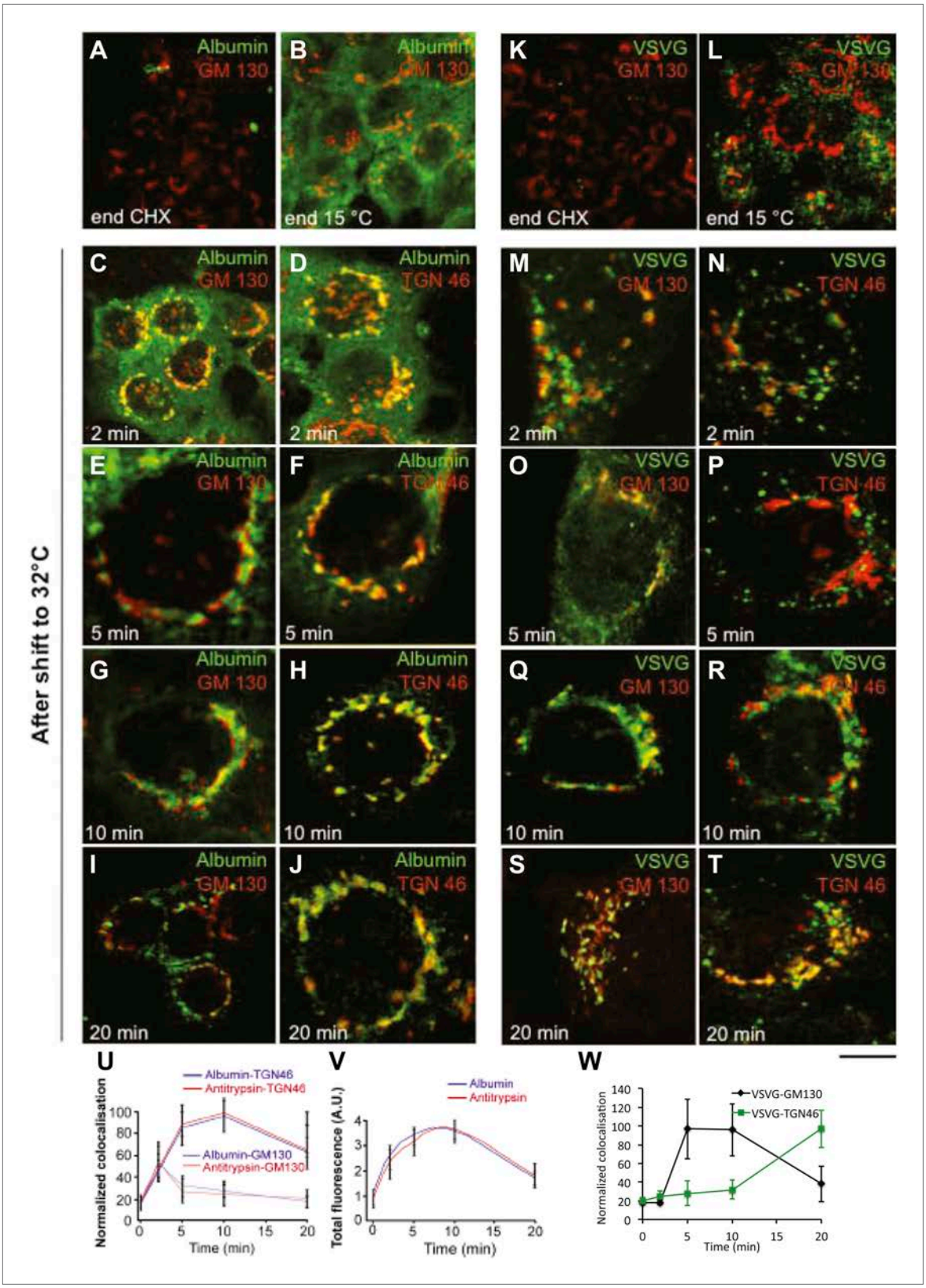

Figure 1—figure supplement 1. Kinetic patterns of synchronised transport of albumin and VSVG through the Golgi stack as determined by immunofluorescence.

DOI: 10.7554/eLife.02009.004

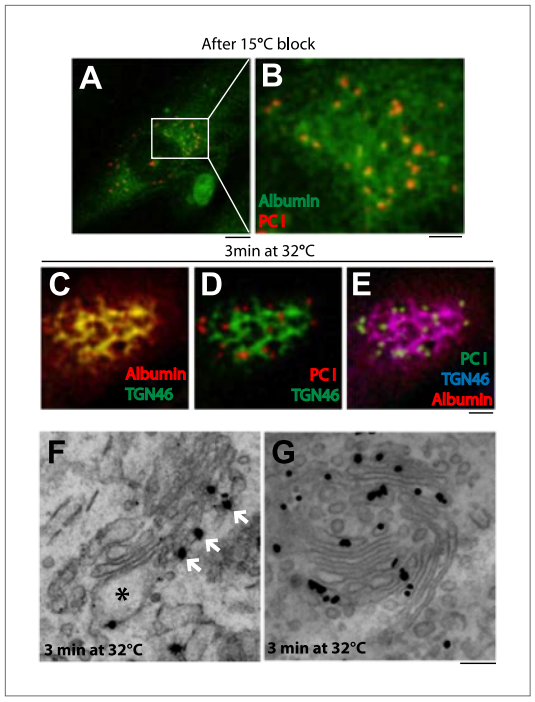

Figure 2. Kinetic patterns of synchronized transport of albumin and PC-I through the Golgi stack. Human fibroblast cells were microinjected in the nucleus with cDNA for albumin and incubated for 2 hr before further treatments. Transport was synchronized according to the CHX/32-15°C protocol and the cells were examined by immunofluorescence and immuno-EM. (**A**) Immunofluorescence localization of albumin and PC at the end of the 15°C block. The area in (**A**) indicated by white rectangle is enlarged in (**B**) (**C**–**E**). Co-localization between albumin (**C**) or PC (**D**) or of both cargoes (**E**) with TGN46, 3 min after release of the block. (**F**–**G**). Localization of PC (**F**) and albumin (**G**) 3 min after release of the 15°C block by immuno-EM. PC (indicated by *) localizes selectively to the cis-cisterna. The cis-side of the Golgi is revealed by the presence of GM130 labeled by immuno-nanogold technique (indicated by white arrows) (**F**). Albumin labeled by immuno-nanogold technique (black dots) shows a diffuse localization throughout the Golgi complex (**G**). Bars: 5 μm (**A**), 2 μm (**B**–**E**), 125 nm (**E** and **F**).

DOI: 10.7554/eLife.02009.005

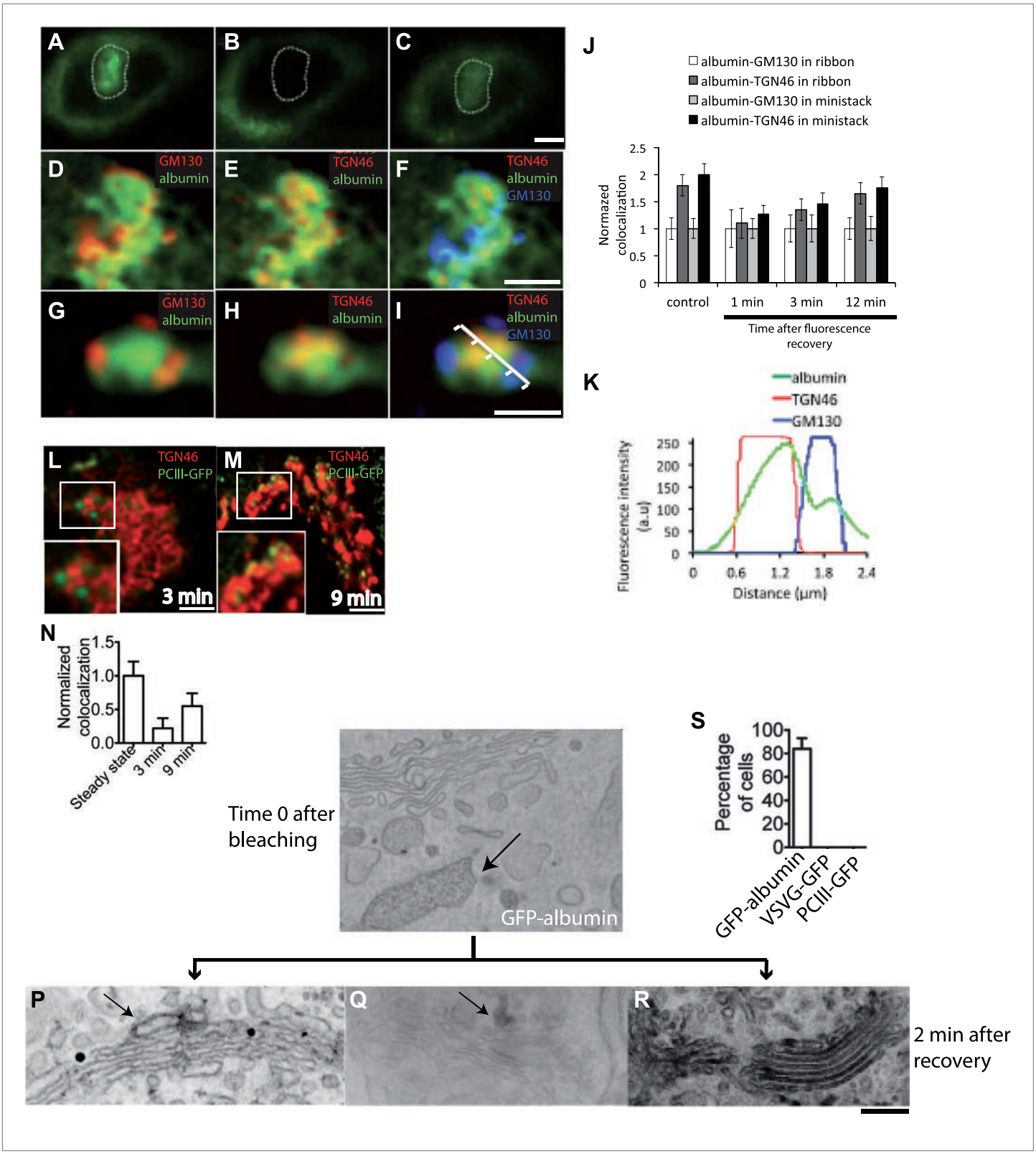

Figure 3. Kinetic patterns of transport of GFP-albumin, VSVG-GFP and PC-III-GFP through the Golgi stack under steady-state conditions. HeLa cells were transfected with GFP-albumin (**A**–**K**) or PC-III-GFP (**L**–**N**). After 16 hr of transfection, the Golgi area was bleached, and entry of these cargoes from the unbleached periphery (ER) into the Golgi area was monitored by FRAP. The cells were then fixed at different time points, stained for GM130 and

Figure 3. Continued on next page

Figure 3. Continued

TGN46, and re-localized for analysis of co-localization of the GFP-tagged cargoes with these Golgi markers. (**A**–**C**) Bleaching of the Golgi area, as delineated by the dotted line, with post-bleaching recovery for 1 min (**C**). (**D**–**F**) Detail of the same Golgi area shown in (**C**), showing co-localization of GFP-albumin (green) with GM130 (**D**, red), or TGN46 (**E**, red) or both (**F**: GM130, blue; TGN46, red). (**G**–**I**) Similar experiments carried out on a nocodazole-induced Golgi ministack ('Materials and methods'), with 1-min post-bleaching co-localization of GFP-albumin (green) with GM130 (**G**, red) or TGN46 (**H**, red) or both (GM130, blue and TGN46, red) (**I**). (**J**) Quantification of the degree of co-localization of GFP-albumin with GM130 and TGN46 at different time points after bleaching, as illustrated in (**A**–**F**). These data are expressed by normalizing the degree of co-localization of GFP-albumin in the TGN46 area to that of albumin in the GM130 area (set to 1). (**K**) Line scan along the arrow across the Golgi ministack shown in (**I**). The fluorescence intensities from representative points along the distance were plotted. (**L** and **M**) Cells were transfected with PC-III-GFP. The Golgi area (within the dotted line) was bleached, and the time course of entry of PC-III-GFP to the TGN was monitored. The cells were fixed and stained for TGN46 at 3 min (**L**) and 9 min (**M**) post-bleach, and the overlap between PC-III-GFP with TGN46 was examined. (**N**) Quantification of data in (**L** and **M**), expressed as mean ± SD from at least three independent experiments. (**O**–**S**) To ascertain the earlier observations of rapid filling of the Golgi stack by GFP-albumin (**A**–**F**), we resorted to electron microscopy. HeLa cells were transfected with GFP-albumin (**O** and **R**) or VSVG-GFP (**P**) or PC-III-GFP (**Q**). The Golgi localized fluorescence was bleached as before (time 0; **O**) and entry of cargo into the Golgi area monitored by FRAP and the cells fixed 2 min after recovery. The GFP fluorescence was then converted to a signal visible at the EM by photooxidation (see 'Photooxidation' under 'Materials and methods' section) using Diaminobenzidine (DAB). The DAB product is indicated by arrows. At time 0 the DAB product is present only in the ER with Golgi devoid of staining (**O**). After 2 min of fluorescence recovery, both VSVG-GFP (**P**) and PC-III-GFP (**Q**) are restricted to the cis-side of the Golgi, while GFP-albumin (**R**) is present throughout the Golgi. In the case of VSVG-GFP, DAB precipitate is visible outside of the Golgi cisternae because GFP is attached to the cytosolic tail of VSVG. In addition, nanogold labeling for Mannosidase II was done in (**P**) that marks the medial-part of the Golgi. The time 0 image shown is from cells expressing GFP-albumin; similar staining was obtained from both VSVG-GFP and PC-III-GFP expressing cells at time 0. (**S**) The percentage of cells that showed DAB product throughout the Golgi 2 min after recovery was calculated and presented as mean ± SD. Bar: 2 μm (**A**–**M**), 220 nm (**O**–**R**).

DOI: 10.7554/eLife.02009.006

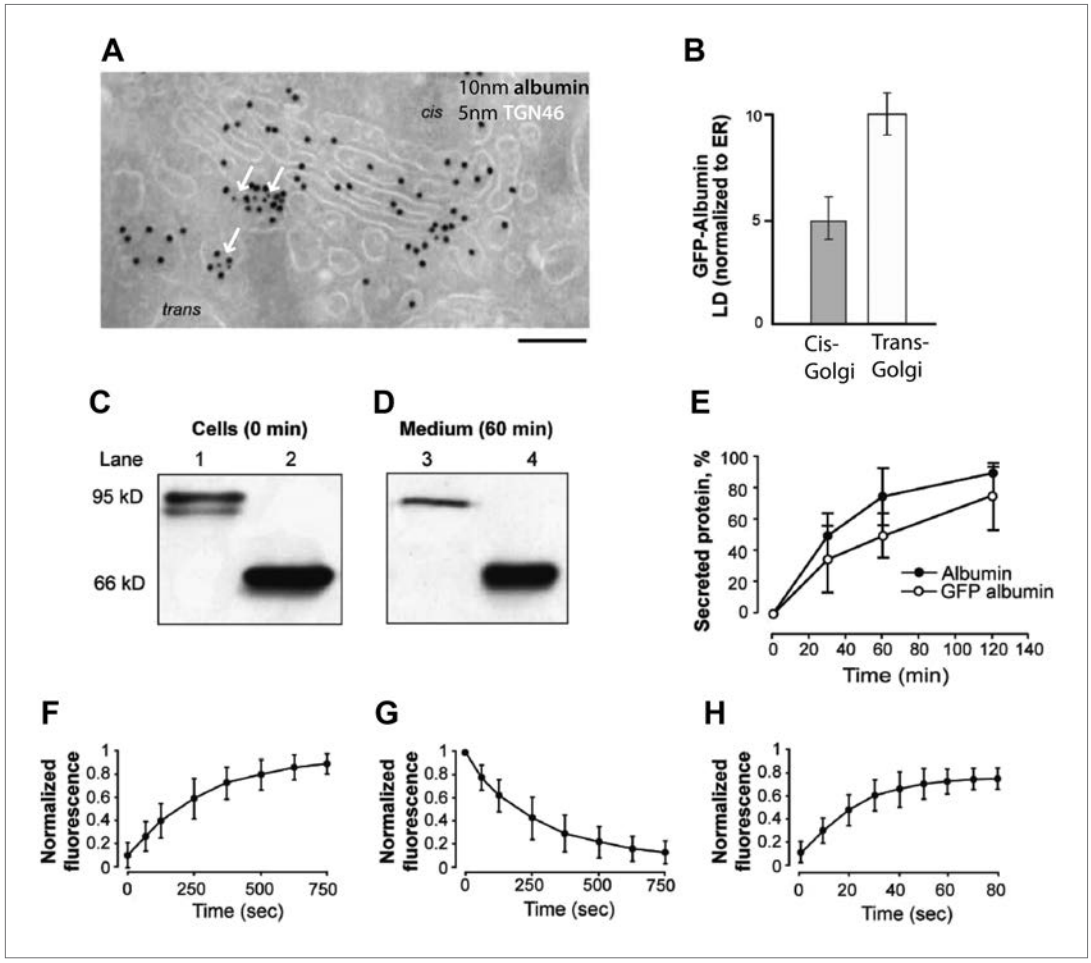

Figure 3—figure supplement 1. Localization, transport behavior, and dynamics of GFP-albumin at steady-state.

DOI: 10.7554/eLife.02009.007

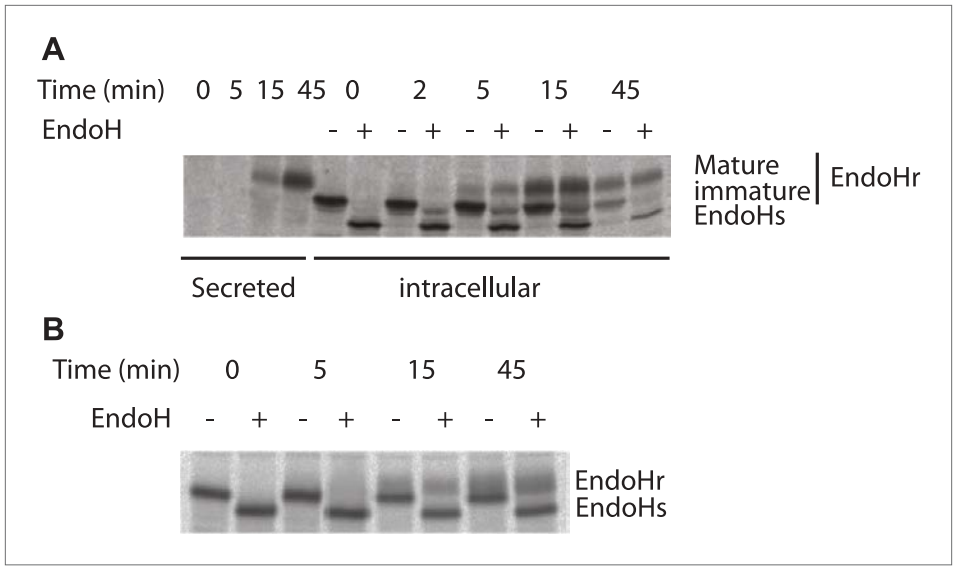

Figure 3—figure supplement 2. Kinetics of antitrypsin processing by Golgi enzymes reflects its fast kinetics of transport.

DOI: 10.7554/eLife.02009.008

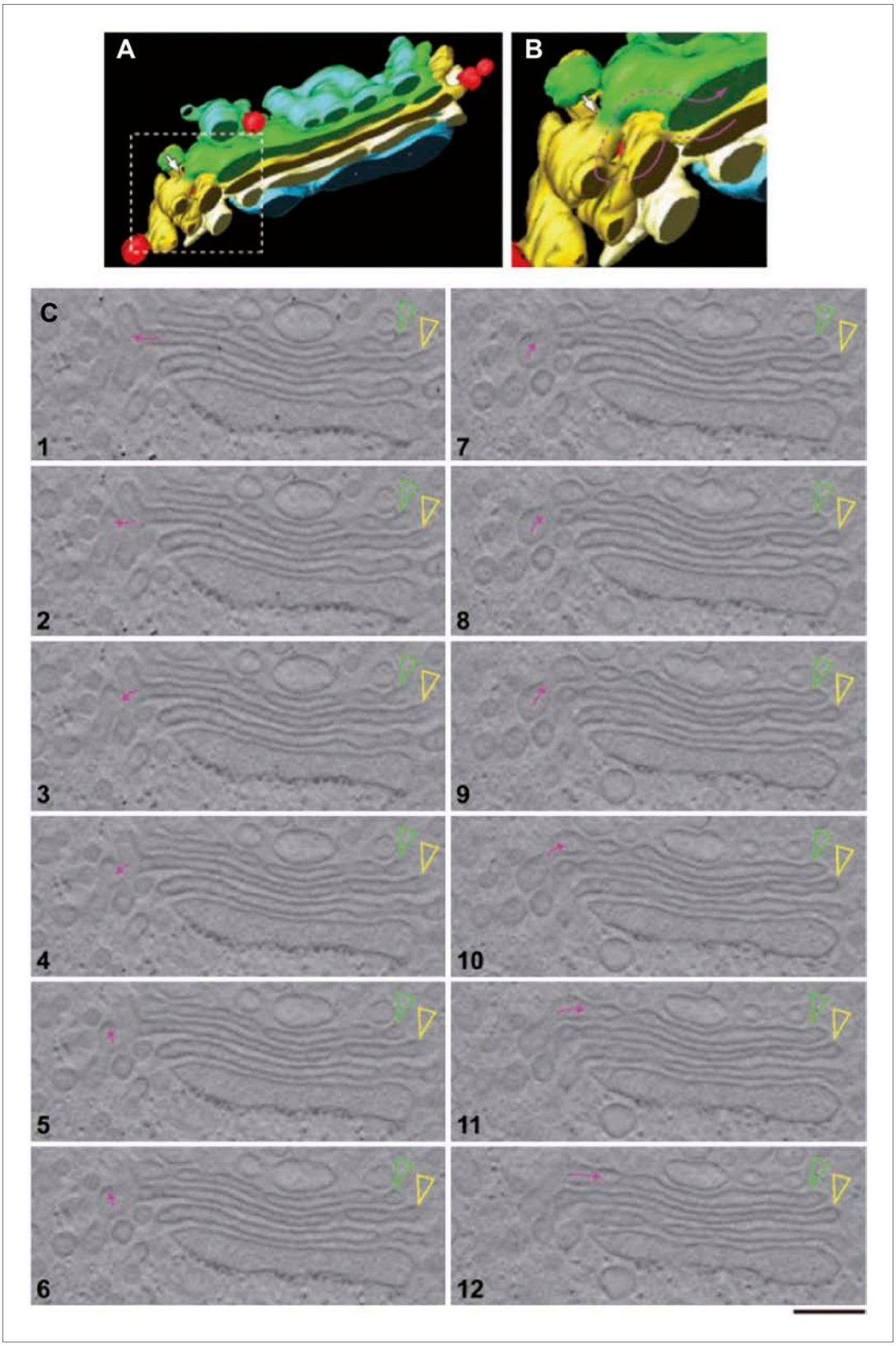

Figure 4. EM tomography facilitates the visualization of convoluted intercisternal tubules. HepG2 cells were high-pressure frozen and prepared for EM tomography ('Materials and methods'). (**A** and **B**) Tomographic model of a stack from a 200-nm-thick section containing an intercisternal connection. Detail of **A** shown in **B**; note the

Figure 4. Continued on next page

Figure 4. Continued

complexity of the convoluted connection (follow the arrow to identify the continuity). (**C**) A gallery of tomographic digital slices (panels 1–12) used to construct the model in (**A** and **B**) shows a convoluted intercisternal connection, with the small arrow following the connection, and the arrowheads showing the two cisternae that are connected. Note the complexity of the connection, which would be nearly impossible to detect in traditional thin sections. See ***Video 1*** for facilitated visualization of the continuity. Bar: 150 nm.

DOI: 10.7554/eLife.02009.009

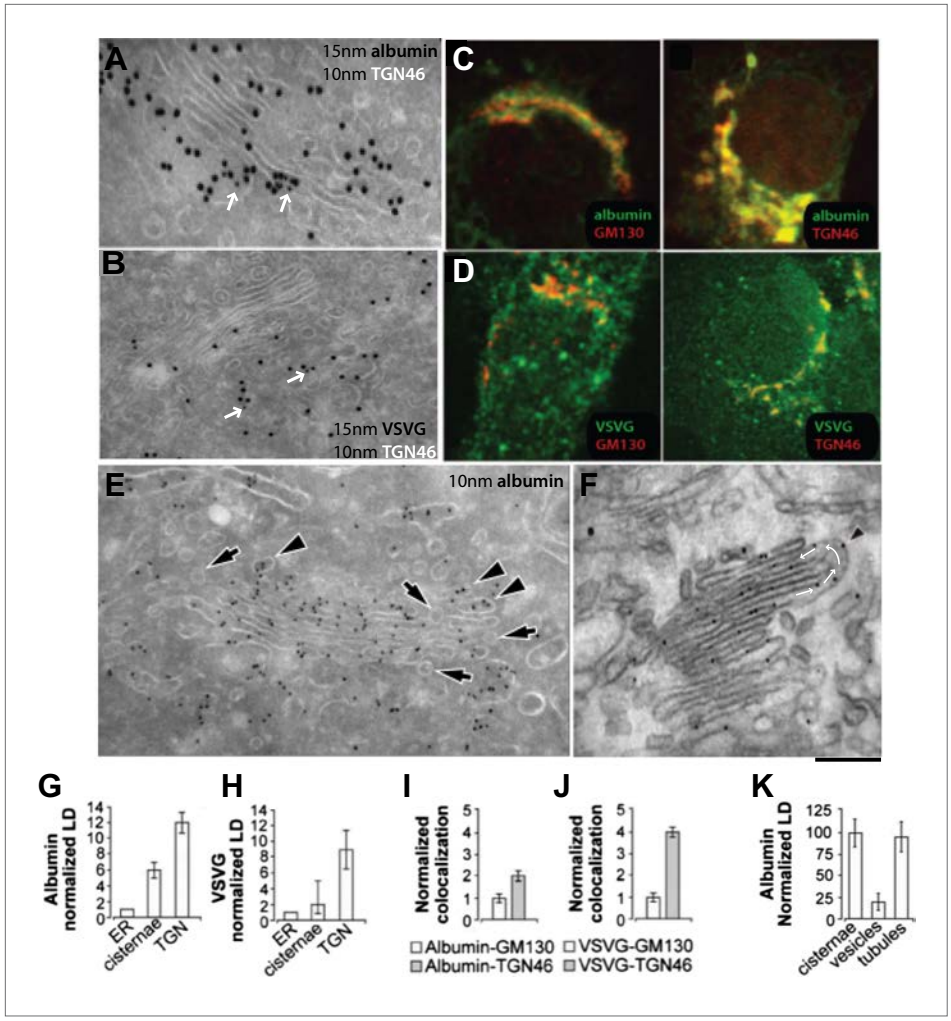

Figure 5. Albumin distribution in Golgi cisternae, vesicles and tubules in HepG2 cells. (**A**–**D**) Albumin and VSVG distribution in the ER, Golgi stack and TGN (**A** and **B**, immuno-EM; **C** and **D**, immunofluorescence). White arrows in (**A** and **B**) indicate TGN46 labeling. For quantification see (**G**–**J**). (**E**) Albumin distribution in cisternae, vesicles (50–60 nm wide round profiles near the Golgi stack; arrows) and tubules (tubular–ovoid profiles; arrowheads), by immuno-EM. (**F**) Albumin present in a connected cis-trans vertical tubule, as visualized by the immuno-nanogold technique. Arrowhead indicates albumin and white arrows highlight the intercisternal connection. For quantification see (**K**). (**G** and **H**) Quantification of labeling density (LD) of albumin and VSVG by immuno-EM, normalized to ER labeling. (**I** and **J**) Quantification of co-localization (as described in 'Materials and methods') of the cargoes with GM130 (cis-Golgi) and TGN46 (TGN) markers by immunofluorescence, normalized to their co-localization with GM130. (**K**) Quantification of distribution of albumin in cisternae, peri-Golgi vesicles and tubules expressed as LD. Bars: 120 nm (**A**), 210 nm (**B**), 7.5 μm (**C** and **D**), 250 nm (**E** and **F**).

DOI: 10.7554/eLife.02009.011

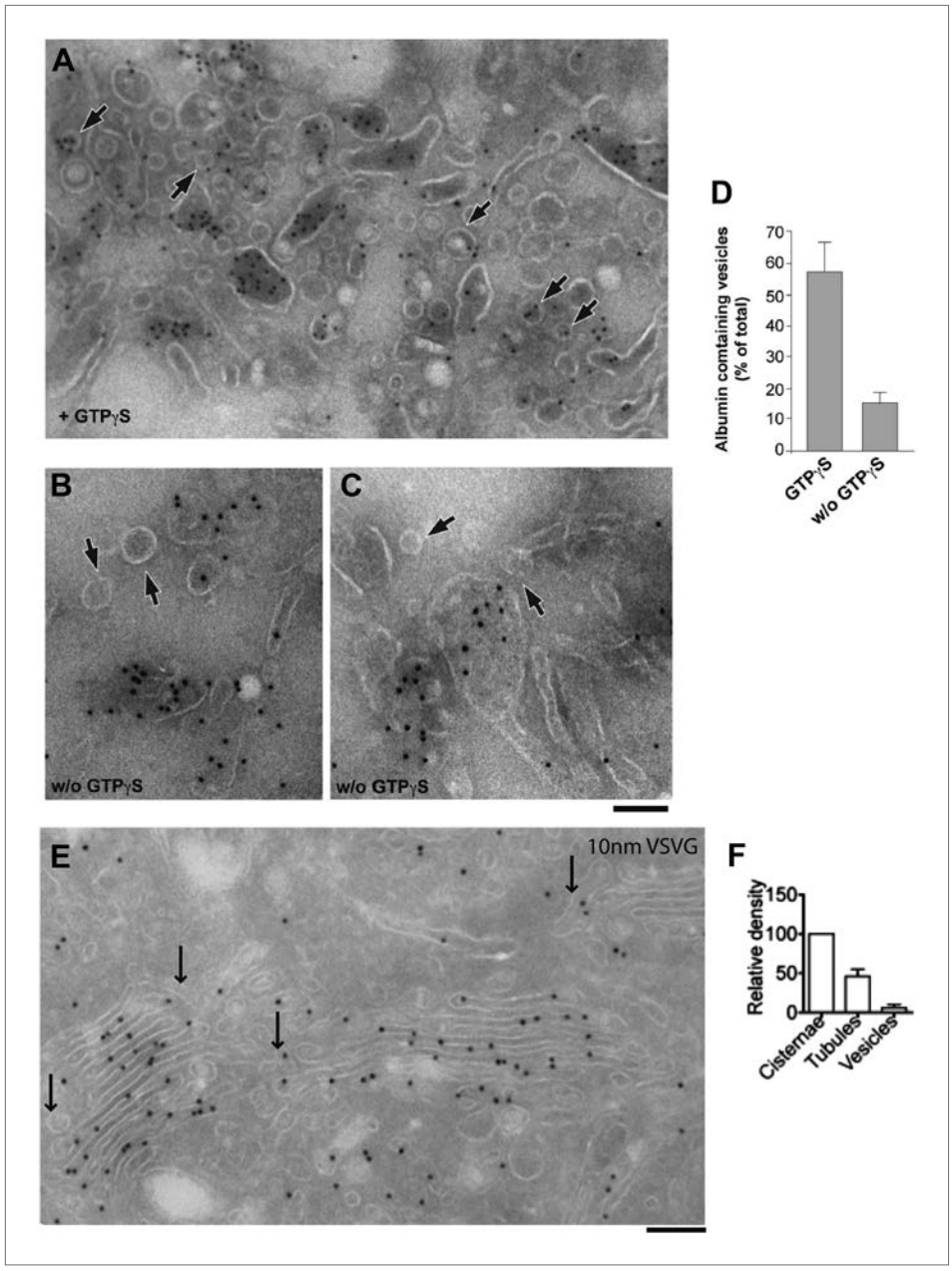

Figure 5—figure supplement 1. Distribution of cargoes in COPI vesicles.

DOI: 10.7554/eLife.02009.012

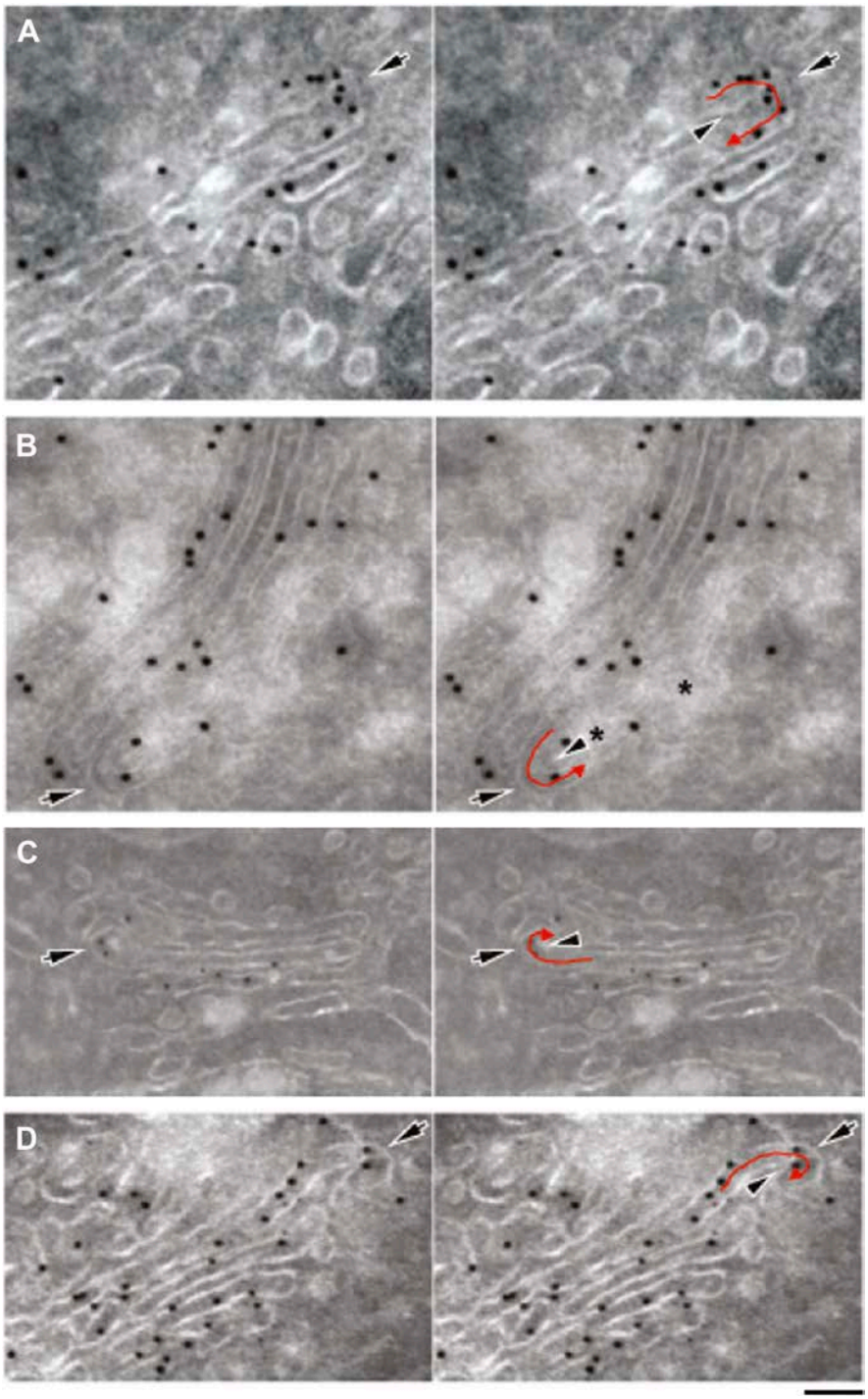

Figure 5—figure supplement 2. Gallery of cryo-immuno-gold EM images indicating the presence of albumin in intercisternal tubules.

DOI: 10.7554/eLife.02009.013

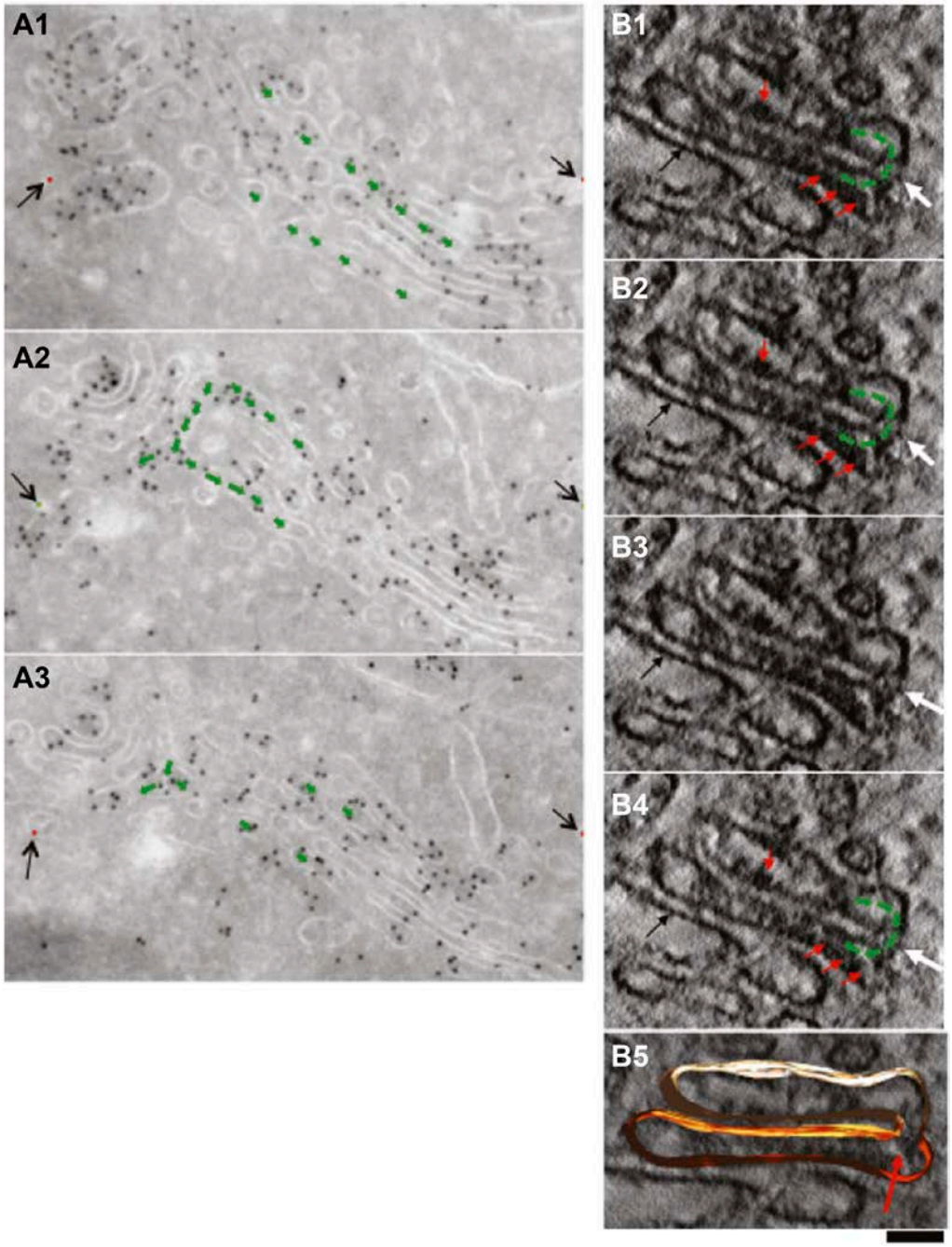

Figure 5—figure supplement 3. Presence of albumin in intercisternal tubules revealed by serial sectioning followed by cryo-immuno-gold EM and DAB photooxidation followed by tomography.
DOI: 10.7554/eLife.02009.014

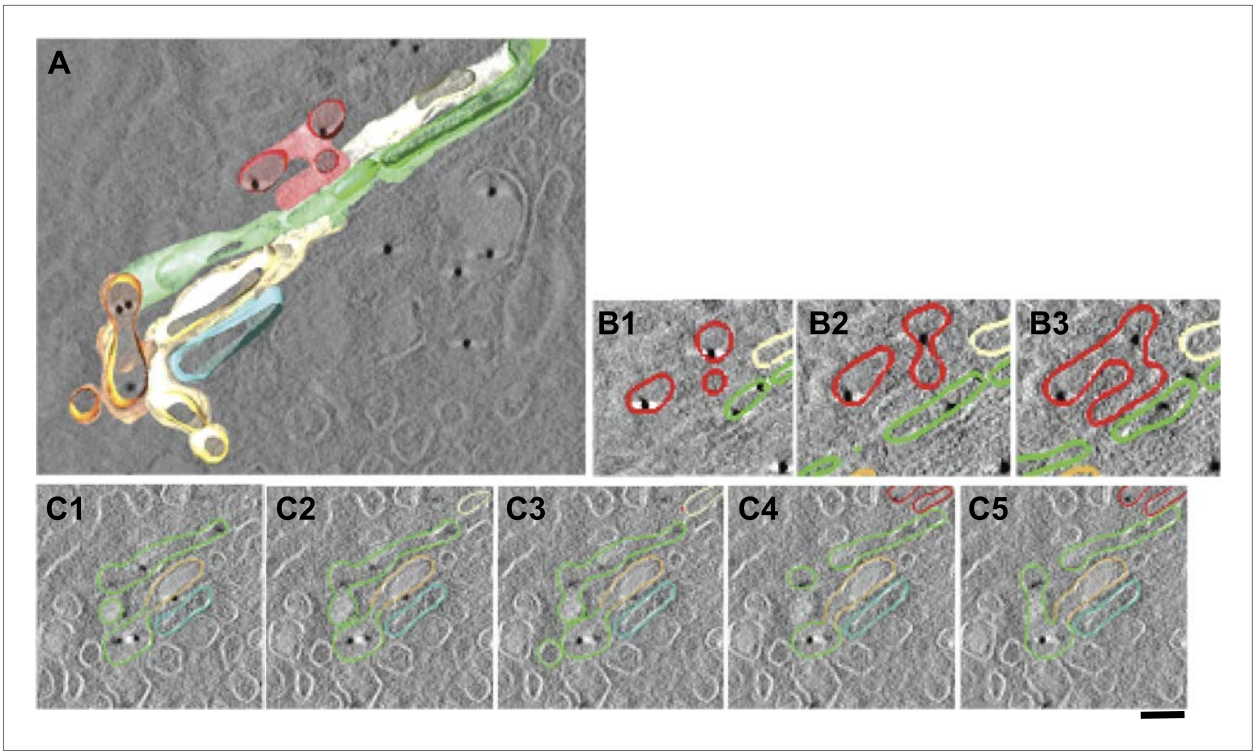

Figure 5—figure supplement 4. Presence of albumin in intercisternal tubules revealed by cryo-immuno EM followed by tomography.
DOI: 10.7554/eLife.02009.015

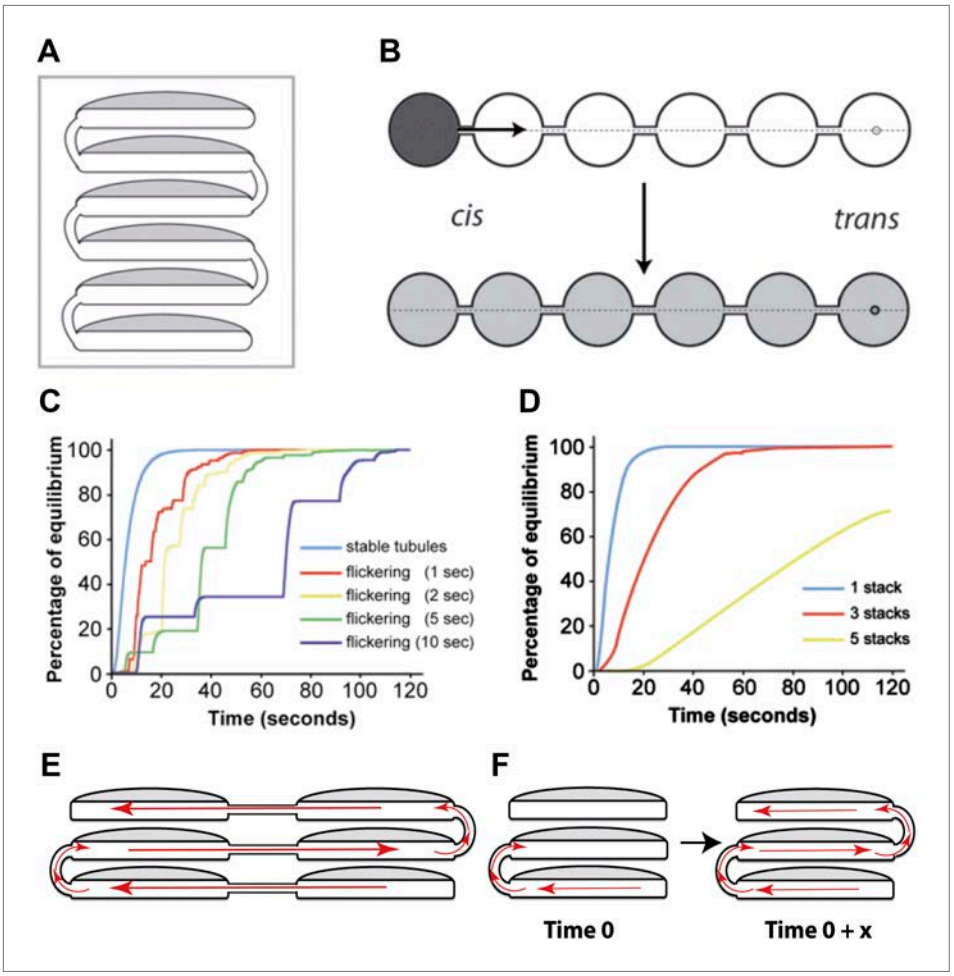

Figure 6. Computational simulations of intra-Golgi transport of albumin by diffusion via intercisternal tubules. (**A**) The Golgi stack was modeled as a system of six circular cisternae connected in series by five (one per pair of cisternae) vertical cylindrical tubules. (**B**) The same stack drawn in a 'distended' disposition. The size of the cisternae was set to 1.5 μm diameter and 30 nm thickness, and the diameter and length of the tubules to 30 nm and 100 nm, respectively. The simulations started with the first cisterna (*cis*) filled with albumin (black shading) and all of the others empty (no shading). Albumin was then allowed to diffuse through the connections until it asymptotically reached equilibrium (gray shading in all cisternae). The variations with time in the albumin concentrations in the other cisternae were calculated for the center of the cisternae (see below). For wider tubule diameters of 60 nm and 120 nm, the 90% threshold of equilibrium was reached after 7.8 s and 6.8 s compared to 14.9 s for the 30 nm diameter. For shorter and longer tubules of 30 nm diameter with 50 nm and 150 nm lengths, the 90% threshold of equilibrium was reached after 11.4 s and 19.1 s. When assuming a system composed only of four circular cisternae, the 90% threshold of equilibrium in the fourth cisternae was reached after 3.4 s (60 nm diameter, 100 nm length) and 3.0 s (120 nm diameter, 100 nm length) compared to 6.4 s for the 30 nm diameter tubules. For shorter and longer tubules of 30 nm diameter with 50 nm and 150 nm lengths, the 90% thresholds of equilibrium were reached after 5.0 s and 8.4 s. (**C** and **D**) Time-courses of the equilibration process with different Golgi configurations and with stable or transient (flickering) intercisternal tubular connections. (**C**) One stack of six cisternae connected by one stable tubule per pair of adjacent cisternae (five connections in all), or by one transient tubule per pair of adjacent cisternae. The tubules were set to be open for 50% of their time, with equal average open and closed times as indicated. In these simulations, the individual tubules opened and closed randomly. (**D**) Simulation of diffusion based albumin transport in Golgi ribbons of one (blue), three (red), or five (yellow) stacks (each with 6 cisternae). The ribbons were completely connected horizontally by tubules joining adjacent cisternae. The total number of connections was five in all cases. For instance, the three-stack ribbon had one or two connections per stack. Nevertheless, complete equilibration was reached in less than 60 s. (**E**) Possible diffusion route of a soluble cargo through the Golgi ribbon with three stacks where the longitudinal tubules connecting the isolated

Figure 6. Continued on next page

Figure 6. Continued

stacks compensate for the vertical connectivity gaps. (**F**) Diffusion of a soluble cargo across a stack through transient intercisternal tubules.

DOI: 10.7554/eLife.02009.016

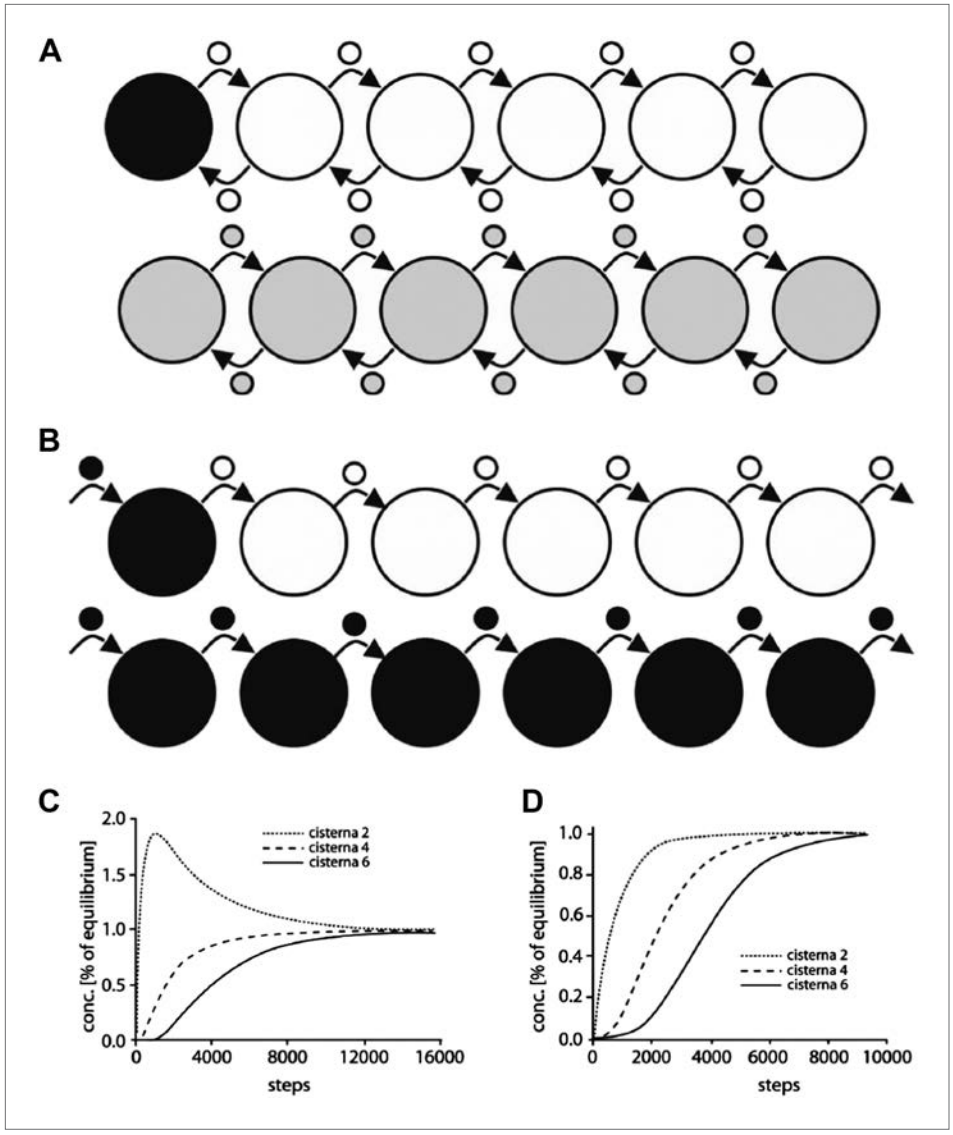

Figure 6—figure supplement 1. Computational simulation of the intra-Golgi equilibration of albumin argues against the classic vesicular transport model.

DOI: 10.7554/eLife.02009.017

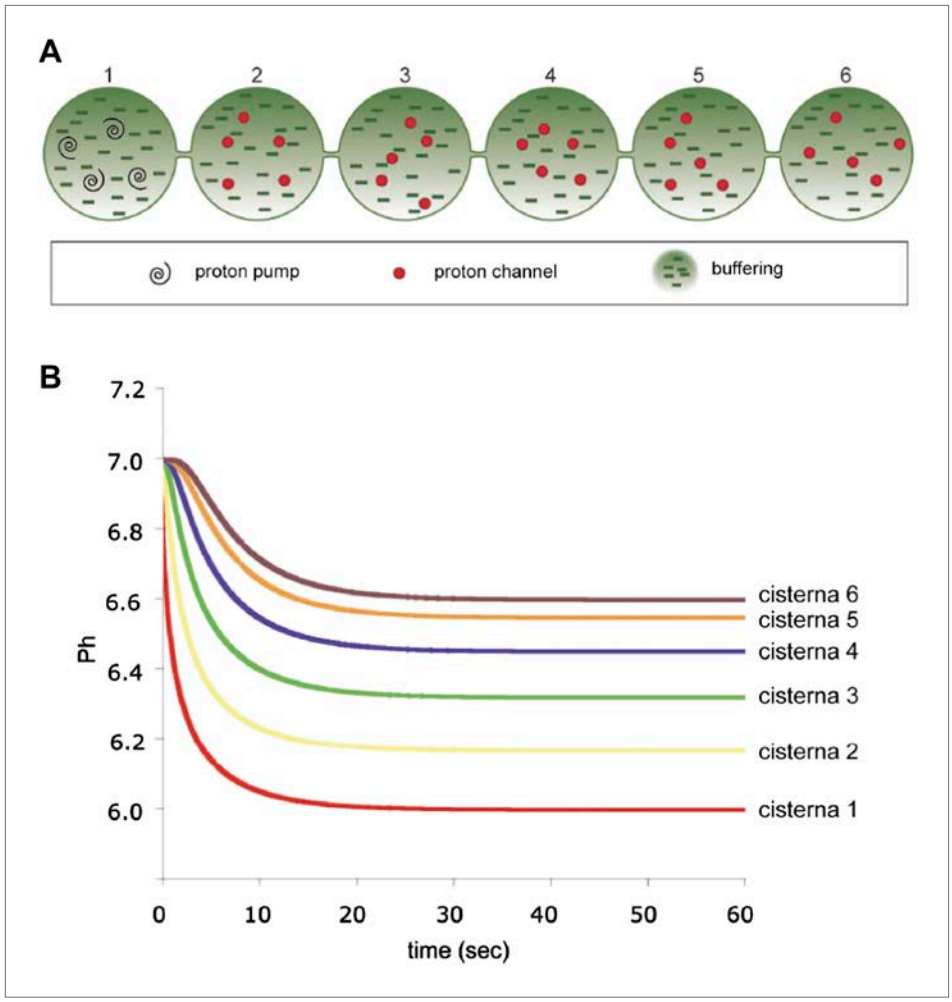

Figure 6—figure supplement 2. Computer-simulated model of the formation of a pH gradient between continuous *cis*- and *trans*-Golgi cisternae.

DOI: 10.7554/eLife.02009.018